Infrared Spectra and Density Functional Calculations for OMCO, OM−(η^2-CO), $OMCO^+$, and $OMOC^+$ (M = V, Ti) in Solid Argon

Mingfei Zhou and Lester Andrews*

Department of Chemistry, University of Virginia, Charlottesville, Virginia 22901

Received: November 11, 1998; In Final Form: January 26, 1999

Laser-ablated V and Ti atoms react with CO_2 molecules to give primarily the insertion products, OMCO and $O_2M(CO)_2$, which have been isolated in a solid argon matrix. Photoisomerization of OMCO molecules to form the side-bonded OM−(η^2-CO) isomers and photoionization to give the $OMCO^+$ and $OMOC^+$ cations proceed upon mercury arc photolysis. The product absorptions were identified by isotopic substitution and density functional calculations of isotopic frequencies.

Introduction

Carbon dioxide is known to contribute to the greenhouse effect. The recycling of CO_2 generated in industrial emission to useful chemical compounds is important from an environmental point of view. Investigation of reactions of transition metal atoms with CO_2 can provide useful information toward understanding the mechanism of catalytic activation of CO_2 in transition metal complexes.[1] The interaction of CO_2 and transition metal centers has been studied both experimentally[2−11] and theoretically.[12−16] Complexes with first-row transition metals have been studied in solid CO_2,[2] and the reactions of laser-ablated Sc, Ti, Cr, Mo, and W atoms with CO_2 in excess argon have been investigated in this laboratory.[3−5] These experiments indicate that early transition metals insert into CO_2 to form OMCO molecules, while the later metals form 1:1 complexes.

The interaction between several first-row transition metal cations and CO_2 has also been studied in the gas phase.[5−11] Different M^+CO_2 structures have been proposed and binding energies were measured. A theoretical study of first-row transition metal M^+-CO_2 and OM^+CO systems shows that the M^+OCO structure is the most favorable coordination for CO_2, but for early transition metals, the inserted OM^+CO structure is more stable than the M^+OCO isomer due to the strong terminal MO^+ bond that is formed.[13]

In this paper, we present the study of the reaction of laser ablated V and Ti atoms with CO_2 molecules. We will show that insertion to form OMCO is the primary reaction, and that photoisomerization to the OM−(η^2-CO) isomer and photoionization to the $OMCO^+$ and $OMOC^+$ cations proceed on visible and ultraviolet photolyses, respectively.

Experimental Section

The experiment for laser ablation and matrix isolation spectroscopy has been described in detail previously.[17] Briefly, the Nd:YAG laser fundamental (1064 nm, 10 Hz repetition rate with 10 ns pulse width) was focused on the rotating V and Ti metal targets (Johnson Matthey, 99.9% and Goodfellow, 99.99%). Laser-ablated metal atoms were co-deposited with carbon dioxide (0.5%-1.0%) in excess argon onto a 12 K CsI cryogenic window at 2−4 mmol/h for 1−2 h. Carbon dioxide (Matheson) and isotopic $^{13}C^{16}O_2$ and $^{12}C^{18}O_2$ (Cambridge Isotopic Laboratories) and $^{12}C^{16}O_2 + {}^{13}C^{16}O_2$, $^{12}C^{16}O_2 + {}^{12}C^{16}O^{18}O + {}^{12}C^{18}O_2$ mixtures were used in different experiments. FTIR spectra were recorded at 0.5 cm^{-1} resolution on a Nicolet 750 spectrometer with 0.1 cm^{-1} accuracy using an MCTB detector. Matrix samples were annealed at different temperatures and subjected to different wavelength region photolyses using a medium-pressure mercury arc (Philips, 175w) lamp and glass filters.

Results

FTIR spectra of the V + CO_2/Ar, Ti + CO_2/Ar and Ti + CO_2/Ne systems and DFT calculations of expected product molecules will be presented.

V + CO_2/Ar. Infrared spectra of laser-ablated V atoms co-deposited with 0.5% CO_2 in excess argon gave a number of new absorptions which are listed in Table 1. After deposition, strong bands at 1881.1 and 974.8 cm^{-1} together with CO absorption at 2138.3 cm^{-1}, CO_2^- species absorptions at 1657.0 and 1652.7 cm^{-1},[18,19] and weak absorptions at 2150.6, 2115.4, 1984.5, 1851.7 and 942.8 cm^{-1} were observed. Annealing to 20 and 25 K slightly decreased the 1881.1, 974.8 cm^{-1} and 1657.0, 1652.7 cm^{-1} absorptions, slightly increased the band sets at 2150.6, 2115.4, 942.8 cm^{-1} and 1984.5, 1851.7 cm^{-1}, and produced $C_2O_4^-$ absorptions at 1856.7 and 1184.7 cm^{-1}.[19] Mercury arc photolysis almost doubled the 1881.1 and 974.8 cm^{-1} bands and the band set at 2150.6, 2115.4, 942.8 cm^{-1}, and produced three new band sets at 2205.4, 1020.0, 2059.3, 1029.6 cm^{-1} and 1516.1, 990.0 cm^{-1}. Further annealing increased the 2150.6, 2115.4, 942.8 cm^{-1} band set and decreased all other absorptions.

Similar spectra were obtained using isotopic $^{13}C^{16}O_2$ and $^{12}C^{18}O_2$ samples; spectra for $^{13}CO_2$ are shown in Figure 1. No shifts were observed for bands in the 1050−900 cm^{-1} region in the $^{13}C^{16}O_2$ experiments, while the bands in the upper region show isotopic shifts. In the $^{12}C^{18}O_2$ experiment, all the product absorptions exhibited isotopic shifts as listed in Table 1. Mixed $^{12}C^{16}O_2 + {}^{13}C^{16}O_2$ and $^{12}C^{16}O_2 + {}^{12}C^{18}O_2$ experiments were also done; spectra in selected regions are shown in Figure 2 for the former mixture, and the isotopic counterparts are listed in Table 1.

10.1021/jp9844009 CCC: $18.00
Published on Web 03/13/1999

TABLE 1: Infrared Absorptions (cm^{-1}) from Co-Deposition of Laser-Ablated Vanadium Atoms with CO_2 Molecules in Excess Argon at 10 K

$^{12}C^{16}O_2$	$^{13}C^{16}O_2$	$^{12}C^{18}O_2$	$^{12}C^{16}O_2 + {}^{13}C^{16}O_2$	$^{12}C^{16}O_2 + {}^{12}C^{18}O_2$	*R*(12/13)	*R*(16/18)	assignment
2344.8	2279.2	2309.7	2344.8, 2279.2	2344.8, 2309.7	1.02878	1.01520	CO_2
2339.0	2273.6	2304.1	2339.0, 2273.6	2339.0, 2304.1	1.02876	1.01515	CO_2
2205.4	2156.2	2153.9	2205.4, 2156.1	2205.5, 2153.9	1.02282	1.02391	$OVCO^+$
2203.3	2154.1	2151.9	2203.3, 2154.1	2203.4, 2152.0	1.02284	1.02389	$OVCO^+$ site
2150.6	2102.3	2100.9			1.02297	1.02366	$O_2V(CO)_2$, ν_s
2143.0	2095.8	2092.0	2143.0, 2095.8	2143.0, 2092.0	1.02252	1.02438	$(CO)_x$
2138.3	2091.1	2087.2	2138.3, 2091.1	2138.3, 2087.3	1.02257	1.02448	CO
2121.9	2074.8	2072.1			1.02270	1.02403	$O_2V(CO)_2$ site
2115.4	2068.5	2065.7	2115.5, 2079.8, 2068.6	2115.5, 2077.7, 2065.8	1.02267	1.02406	$O_2V(CO)_2$, ν_{as}
2111.9	2065.3	2062.1		2111.9, 2074.6, 2062.2	1.02256	1.02415	$O_2V(CO)_2$ site
2076.9	2031.8	2028.4	2076.9, 2031.8	2076.9, 2028.5	1.02220	1.02391	$VOCO^+$?
2059.3	2013.9	2010.1	2059.2, 2014.0	2059.3, 2010.0	1.02254	1.02448	$OVOC^+$
2037.1	1983.3				1.02713		CO_3
1984.5	1939.2	1939.8	1984.5, 1964.6, 1939.3	1984.5, 1964.2, 1939.8	1.02336	1.02304	$OV(CO)_2$
1881.1	1837.8	1839.5	1881.1, 1837.7	1881.1, 1839.4	1.02356	1.02261	OVCO
1874.3	1831.4	1832.8	1874.4, 1831.3	1874.5, 1832.9	1.02342	1.02264	OVCO site
1857.1	1806.8	1826.8	1856.9, 1806.8	1857.1, 1826.8	1.02784	1.01659	$C_2O_4^-$
1851.6	1810.1	1808.8	1851.7, 1827.4, 1810.2	1851.7, 1826.8, 1809.0	1.02293	1.02361	$OV(CO)_2$
1657.0	1612.9	1629.3	1656.9, 1612.9	1657.0, 1629.3	1.02734	1.01700	CO_2^-
1652.7	1608.8	1625.0	1652.8, 1608.8	1652.7, 1625.0	1.02728	1.01705	$(CO_2^-)(CO_2)_x$
1516.1	1483.0	1480.1	1516.1, 1483.0	1516.1, 1480.2	1.02227	1.02431	OV[CO]
1383.9	1368.9	1339.2	1383.8, 1368.4		1.01096	1.03338	$(CO_2)_x$
1278.4	1255.8	1227.7	1278.4, 1256.6		1.01800	1.04130	$(CO_2)_x$
1274.0	1264.8	1221.7	1274.0, 1268.4, 1264.8		1.00727	1.04281	$(C_2O_4^+)$
1257.0	1248.2	1200.2	1257.0, 1248.2		1.00705	1.04733	CO_4^-
1249.1	1240.6	1192.4			1.00685	1.04755	site
1184.7	1177.3	1130.5	1184.7, 1180.8, 1177.2	1184.7, 1148.3, 1130.5	1.00629	1.04794	$C_2O_4^-$
1029.6	1029.6	985.2	1029.6			1.04507	$OVOC^+$
1020.0	1020.0	976.0	1019.9			1.04508	$OVCO^+$
990.0	990.0	947.5	990.0			1.04485	OV[CO]
988.1	988.1	946.0	988.1			1.04450	OV[CO] site
974.8	975.0	932.0	974.9	974.8, 932.0		1.04592	OVCO
969.6							OVCO site
951.3	951.2		951.2				$O_2V(CO)_2$, ν_s
949.8	949.6	905.0	949.7			1.04950	$O_2V(CO)_2$ site
944.3	944.4	908.6	944.3			1.03929	$O_2V(CO)_2$ site
942.8	942.8	907.1	942.7	942.8, 906.9		1.03936	$O_2V(CO)_2$, ν_{as}
940.9	940.9	905.0				1.03967	site
938.0	937.9	902.4				1.03945	site
935.8	935.8	899.9				1.03989	VO_2
899.4		867.0				1.03737	VO_2^-
898.2		865.6				1.03766	VO_2^-
691.3	681.0	670.2	691.3, 681.0		1.01512	1.03148	CO_4^-
663.5	644.6	653.5	663.5, 644.6	663.5, 653.5	1.02930	1.01530	CO_2
661.9	643.2	651.9	661.9, 643.2	661.9, 651.9	1.02907	1.01534	CO_2

Ti + CO_2/Ar. The spectra of laser-ablated Ti atoms co-deposited with 0.5% CO_2 in argon are shown in Figure 3, and the absorptions were listed in Table 2. Strong product absorptions were observed at 1866.8, 1864.4 and 952.8, 954.7 cm^{-1} as reported earlier.[3] In addition, weak CO_2^- absorption at 1657.0 cm^{-1},[18,19] $C_2O_4^-$ bands at 1857.1, 1184.7 cm^{-1},[19] absorptions at 990.2, 987.9, 985.6 cm^{-1} due to TiO at different sites, at 917.0 cm^{-1} due to TiO_2,[20] and weak new product bands at 895.2, 882.5, 2193.4, 2188.0 cm^{-1} were observed. Mercury arc photolysis increased weak absorptions at 965.0, 1003.0, 1004.3, 1011.7, 1012.9, 2100.9, 1532.3, and 2065.2 cm^{-1}. Again, isotopic experiments were done; the spectra are shown in Figures 4 and 5 for selected regions, and the absorptions are listed in Table 2.

CCl_4 Doping. Similar experiments were done adding 0.05% CCl_4 to the samples. The initial deposition spectrum reduced the CO_2^- absorptions more than 90% and failed to produced the $C_2O_4^-$ absorptions on annealing. Mercury arc photolysis increased the yield of bands at 2065.2, 1012.9 cm^{-1} and at 2188.0, 1003.0 cm^{-1} relative to the 1866.8, 952.8 cm^{-1} absorptions in the Ti + CO_2 reactions and increased 2205.4, 1020.0 cm^{-1} and 2059.4, 1029.6 cm^{-1} bands relative to the 1881.3, 974.8 cm^{-1} absorptions in the V + CO_2 reactions. Bands characteristic of the CCl_4 system[21−23] were observed at 1036.4, 926.8, and 898.0 cm^{-1}; photolysis decreased the former two and increased the latter band.

Ti + CO_2/Ne. Complementary neon matrix experiments were done for the titanium system using 0.5, 0.15, and 0.05% CO_2 concentrations and a 4 K cryogenic window. Infrared spectra were recorded, and product absorptions are listed in Table 3. The strongest product bands blue-shifted to 1884.0 and 973.1 cm^{-1}, and medium-intensity bands were observed at 2196.3, 1829.5, 906.1, and 891.7 cm^{-1}. The strong CO_2^- band was observed at 1658.2 cm^{-1}, and annealing increased bands at 1852.3 and 1189.2 cm^{-1}, which are the neon matrix counterparts of $C_2O_4^-$.[18,19] In contrast to the argon matrix work, CO_2^+ was observed in solid neon at 1421.6 cm^{-1}.[18] Isotopic counterpart absorptions using $^{13}CO_2$ and $^{12}C^{18}O_2$ reagents are also listed in Table 3. Mixed $^{12}CO_2$ + $^{13}CO_2$ experiments gave a strong 1884.0, 1841.0 cm^{-1} doublet for the upper band, and mixed $^{12}C^{16}O_2$ + $^{12}C^{18}O_2$ samples gave strong 1884.0, 1842.1 cm^{-1} and 973.1, 931.5 cm^{-1} doublets.

Calculations. Density functional calculations were performed for the product molecules expected here using the Gaussian 94 program.[24] The BP86 functional,[25] the 6-311+G* basis sets for C and O atom,[26] and the set of Wachters and Hay for V and Ti

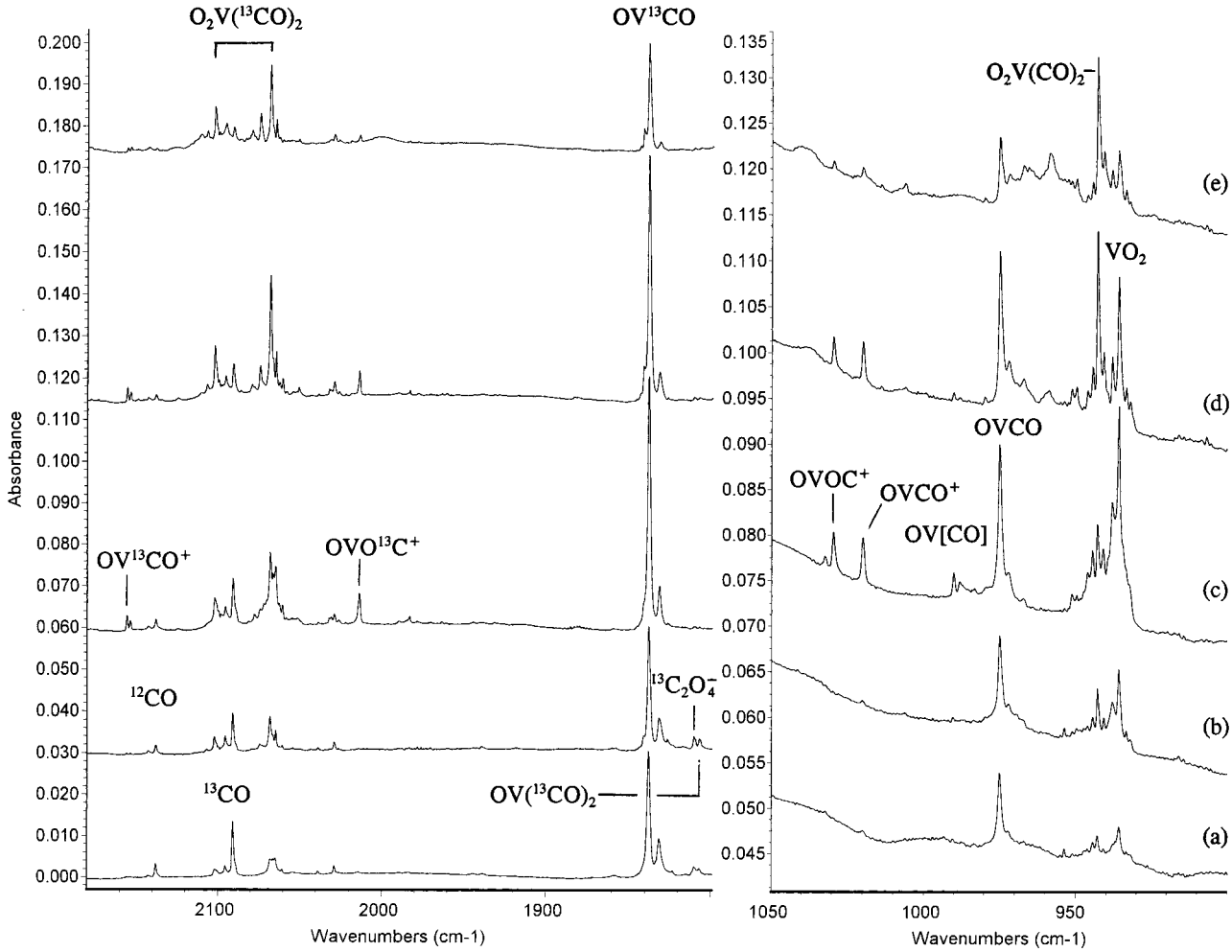

Figure 1. Infrared spectra in selected regions for reaction of laser-ablated V atoms with 0.5% $^{13}CO_2$ in argon during condensation at 12 K: (a) sample co-deposition for 1 h, (b) after annealing to 25 K, (c) after 15 min broadband photolysis, (d) after annealing to 30 K, and (e) after annealing to 35 K.

atoms[27] as provided by Gaussian 94 were used. Five isomers, namely, OVCO, OV−(η^2−CO), V−(η^2−OC)O, V−(η^2−OO)C, and V−CO_2 were calculated, and the results are listed in Table 4. The inserted OVCO isomer was calculated to have a ^{4}A″ ground state; the ^{2}A′ state was only 8.7 kcal/mol higher and cannot be ruled out. The OV−(η^2−CO) isomer has a ^{2}A″ ground state; the ^{4}A″ state converged to OVCO. The ^{4}A″ OVCO state was calculated to be the most stable isomer at this level of theory, followed by the ^{2}A″ OV−(η^2−CO) molecule, which was just 21.8 kcal/mol higher in energy than the ^{4}A″ OVCO molecule.

Four $TiCO_2$ isomers, namely, OTiCO, OTi−(η^2−CO), Ti−(η^2−OO)C, and Ti−(η^2-OC)O were calculated, and the results are listed in Table 5. The Ti−CO_2 and TiOCO isomers were calculated earlier to be higher in energy[16] and are not listed here. The inserted OTiCO molecule was calculated to have a ^{3}A″ ground state, with the ^{1}A′ state being only 6.5 kcal/mol higher. The OTi−(η^2-CO) has a ^{1}A′ ground state, with the ^{3}A″ state being only 3.6 kcal/mol higher in energy. The ^{3}A″ OTiCO state was the most stable $TiCO_2$ isomer followed by the OTi−(η^2-CO) structure, which was 11.2 kcal/mol higher than OTiCO.

Calculations were also done for the $OMCO^+$ cations and the more weakly bound $OMOC^+$ and $MOCO^+$ isomers, and the results are also listed in Tables 4 and 5. The latter is essentially a $MO^+\cdots CO$ complex but is more stable than the $M^+\cdots OCO$ complex[14] for the early transition metal species. The larger molecules $OM(CO)_2$, O_2MCO and $O_2M(CO)_2$ were also investigated, and the results are listed in Tables 6 and 7.

Discussion

The new product molecules will be identified from isotopic shifts and DFT frequency calculations.

OVCO. The 1881.1 and 974.8 cm^{-1} bands were the dominant absorptions on deposition. These two bands exhibit the same annealing and photolysis behavior through all the experiments, suggesting that they are due to different modes of the same molecule. The 974.8 cm^{-1} band showed no carbon-13 isotopic shift, but shifted to 932.0 cm^{-1} using the $^{12}C^{18}O_2$ sample; the 16/18 isotopic ratio (1.0459) is very close to the diatomic VO ratio, and the frequency is slightly lower than that of diatomic molecule in solid argon (983.6 cm^{-1}),[28] suggesting that the 974.8 cm^{-1} band is due to a terminal V−O stretching vibration. The 1881.1 cm^{-1} band shifted to 1837.8 cm^{-1} in the $^{13}C^{16}O_2$ spectra and 1839.5 cm^{-1} in the $^{12}C^{18}O_2$ spectra, the 12/13 isotopic ratio (1.02356) and 16/18 ratio (1.02261) are slightly higher and lower, respectively, than the diatomic C−O ratios; this means that the C atom is vibrating between the O atom and another mass. The doublet structure in both mixed $^{12}C^{16}O_2$ + $^{13}C^{16}O_2$ and $^{12}C^{16}O_2$ + $^{12}C^{18}O_2$ experiments confirmes that only one CO subunit is involved in this mode. Accordingly, these two bands are suitable for assignment to the inserted OVCO molecule.

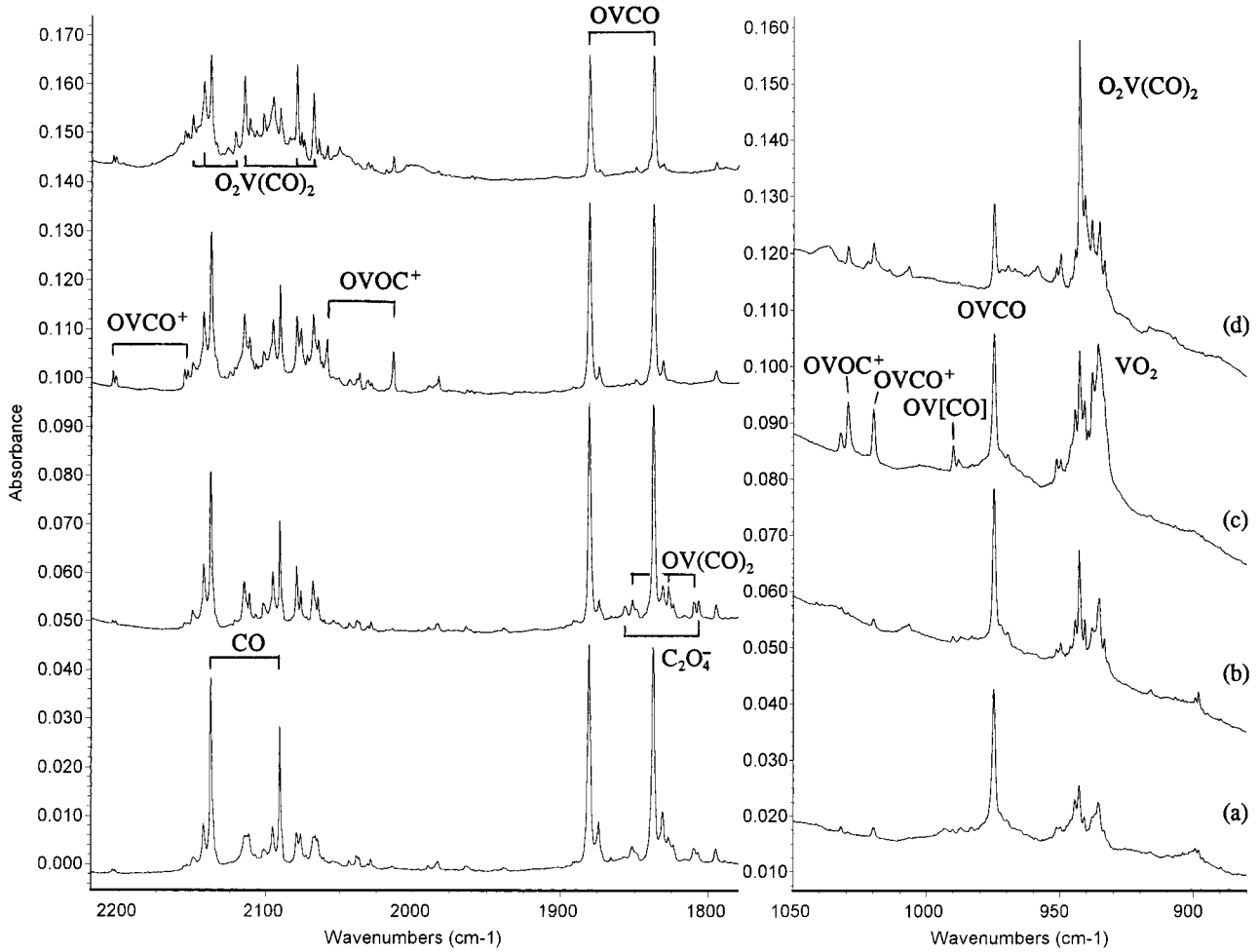

Figure 2. Infrared spectra in selected regions for reaction of laser- ablated V atoms with 0.25% $^{12}CO_2$ + 0.25% $^{13}CO_2$ in argon during condensation at 12 K: (a) sample co-deposition for 1 h, (b) after annealing to 25 K, (c) after 15 min broad-band photolysis, and (d) after annealing to 35 K.

The BP86 calculation predicts that OVCO is the most stable VCO_2 isomer, and both the $^4A''$ and $^2A'$ states are very close in energy. The $^4A''$ state is slightly lower in energy and gave a 1959.8 cm^{-1} C−O stretching frequency and 981.1 cm^{-1} V−O stretching frequency, while the $^2A'$ state gave lower (1893.9 cm^{-1}) C−O and higher (1046.9 cm^{-1}) V−O stretching frequencies. The calculation predicts no coupling between the V−O and C−O stretching modes for both states and gives very close isotopic frequency ratios, as shown in Table 8, so it is difficult to determine which state is the ground state. As will be discussed, the OV−(η^2-CO) molecule, which has a doublet ground state, can be formed by photolysis of the OVCO molecule, suggesting that OVCO has a doublet ground state. Furthermore, scale factors[29] for the BP86 functional are expected to be near 0.99, which suggests that the 1959.8 cm^{-1} frequency calculated for the $^4A''$ state is not compatible with the 1881.1 cm^{-1} observed frequency, but the 1893.9 cm^{-1} frequency calculated for the $^2A'$ state is in excellent agreement.

OTiCO. Similar absorptions at 1866.8 and 952.8 cm^{-1} in the Ti + CO_2 system are assigned to the C−O and Ti−O stretching vibrations of the OTiCO molecule in solid argon, as has been reported earlier.[3] The neon matrix counterparts at 1884.0 and 973.1 cm^{-1} show a modest matrix interaction with OTiCO. The present DFT calculation predicts the OTiCO is the most stable isomer with the $^1A'$ and $^3A''$ states close in energy. The $^3A''$ state gave 1965.1 cm^{-1} C−O stretching and 989.3 cm^{-1} Ti−O stretching vibration freqencies, while the $^1A'$ state gave 1882.1 and 987.7 cm^{-1}. Although the $^3A''$ state was calculated slightly lower in energy, the calculated frequencies and isotopic frequency ratios of the $^1A'$ state match the experimental values much better than the $^3A''$ state (Table 8). This indicates that the $^1A'$ is the ground state, in agreement with another recent theoretical report.[16]

Table 9 compares frequencies for similar early transition metal atom reaction products. The analogous OScCO species has similar frequencies, but OCrCO and OMnCO exhibit much higher carbonyl stretching frequencies.[4,30] This is probably due to lower d-orbital energies on Cr and Mn and less favorable overlap with carbonyl antibonding orbitals.

OV−(η^2-CO). The 1516.1 and 990.0 cm^{-1} bands were produced only on mercury arc photolysis and decreased together on annealing. The 1516.1 cm^{-1} band shifts to 1483.0 and 1480.1 cm^{-1} using the $^{13}C^{16}O_2$ and $^{12}C^{18}O_2$ reagents; the 12/13 isotopic ratio (1.02227) and 16/18 isotopic ratio (1.02431) are very close to values of the diatomic C−O stretching vibration, but the frequency is 622.2 cm^{-1} lower than the diatomic CO frequency, indicating that this is not a terminal C−O stretching vibration. So a side-bonded structure must be considered analogous to the Sc + CO_2 reaction,[5] where a similar 1613.9 cm^{-1} band was assigned to the OSc−(η^2-CO) molecule. In the mixed $^{12}C^{16}O_2$ + $^{13}C^{16}O_2$ and $^{12}C^{16}O_2$ + $^{12}C^{18}O_2$ experiments, only pure isotopic counterparts were observed, so only one CO subunit is involved in this vibration. The associated 990.0 cm^{-1} band showed no carbon-13 isotopic shift; the 16/18 isotopic ratio (1.04485) is just slightly lower than the diatomic VO ratio, while the frequency is only 6.4 cm^{-1} higher, indicating that this

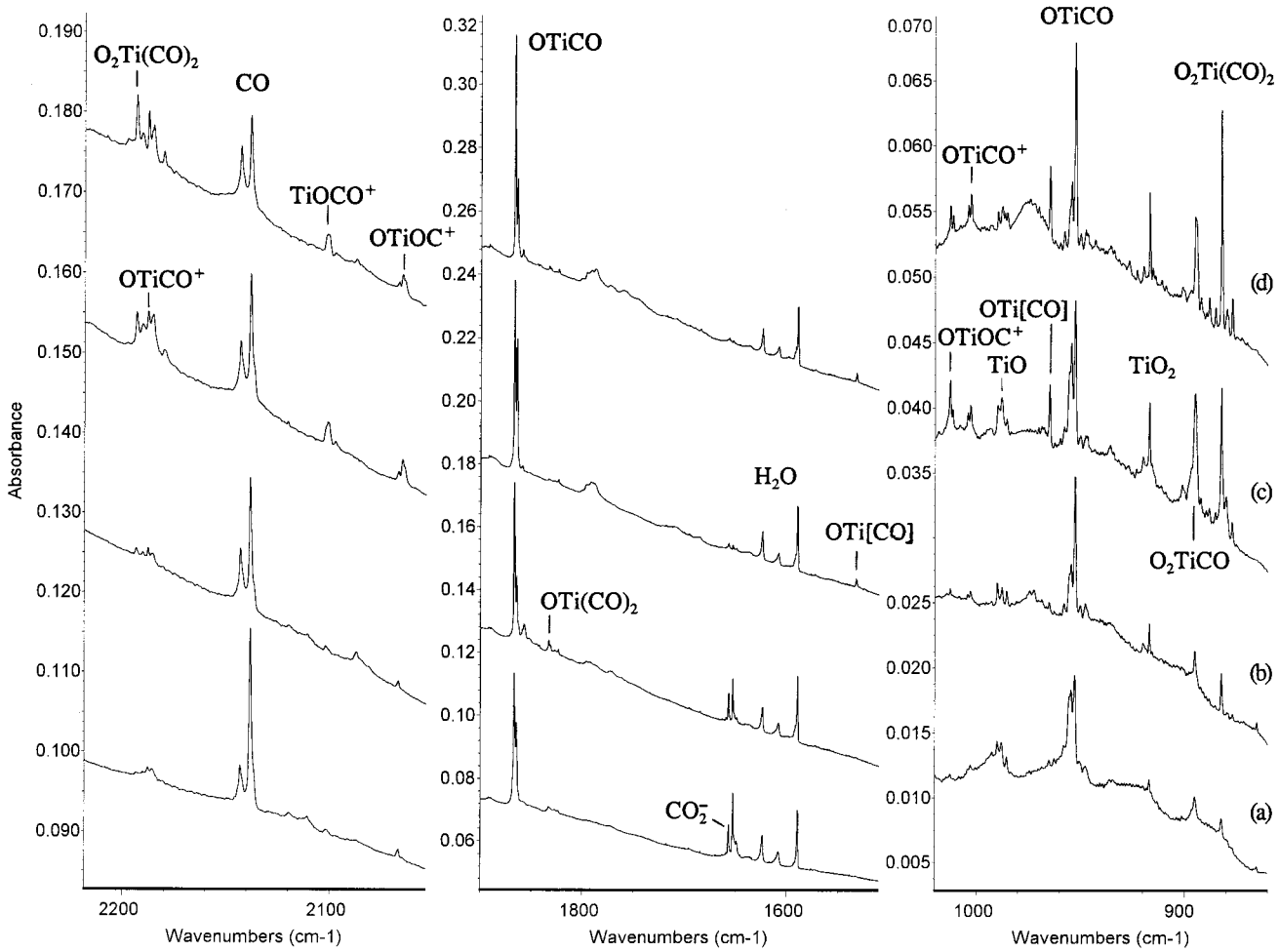

Figure 3. Infrared spectra in selected regions for reaction of laser-ablated Ti atoms with 0.5% CO_2 in argon during condensation at 12 K: (a) sample co-deposition for 1 h, (b) after annealing to 25 K, (c) after 15 min broad-band photolysis, and (d) after annealing to 30 K.

vibration is a terminal V−O stretching mode. These two bands are suitable for assignment to the OV−(η^2-CO) molecule.

This assignment is in good agreement with DFT calculations. The OV−(η^2-CO) molecule has a $^2A''$ ground state, which is about 21.8 kcal/mol higher than the $^4A''$ OVCO isomer. The C−O stretching vibration was calculated at 1489.6 cm^{-1}, slightly lower than the observed value, and the calculated 12/13 ratio, 1.02195, and 16/18 ratio, 1.02561, are very close to the observed values. The V−O stretching frequency was calculated to be 1023.6 cm^{-1}, just 33.6 cm^{-1} above the observed value. The calculated 16/18 isotopic ratio (1.04502) also matches the observed 1.04485 value.

OTi−(η^2-CO). Similar bands at 1532.3 and 965.0 cm^{-1} in the Ti + CO_2 system were also produced on mercury arc photolysis and decreased together on annealing. The 1532.3 cm^{-1} band shifted to 1496.8 and 1496.1 cm^{-1} in $^{13}C^{16}O_2$ and $^{12}C^{18}O_2$ experiments. The 965.0 cm^{-1} band shows no carbon-13 isotopic shift but shifted to 924.5 cm^{-1} using the $^{12}C^{18}O_2$ sample, and the 16/18 ratio (1.04381) characterized this vibration as a terminal Ti−O stretching vibration. The doublet structure in mixed experiments confirmed only one CO subunit in the upper mode and one O atom involved in the lower mode. Accordingly, these two bands are assigned to the C−O stretching and Ti−O stretching vibrations of the side-bonded OTi−(η^2-CO) molecule following the examples of OV−(η^2-CO) and OSc−(η^2-CO).[5] Such bridge-bonded species have only been observed for the early transition metal atoms.

$OVCO^+$. The 1020.0 cm^{-1} band and the doublet at 2205.4, 2203.3 cm^{-1} produced on full-arc photolysis decreased together on subsequent 30 and 35 K annealing. The upper doublet shifted to 2156.2, 2154.1 cm^{-1} and 2153.9, 2151.9 cm^{-1} using $^{13}C^{16}O_2$ and $^{12}C^{18}O_2$ samples, The isotopic 12/13 ratio (1.0228) and 16/18 ratio (1.0239) are very close to the diatomic CO ratios. Only pure isotopic counterparts were observed in both mixed $^{12}C^{16}O_2$ + $^{13}C^{16}O_2$ and $^{12}C^{16}O_2$ + $^{12}C^{18}O_2$ experiments, indicating that only one CO subunit is involved in this vibration. The associated 1020.0 cm^{-1} band showed no carbon-13 displacement but shifted to 976.0 cm^{-1} in $^{12}C^{18}O_2$ spectra; the 1.04508 isotopic 16/18 ratio indicates that this is a terminal V−O stretching vibration. Again, the doublet in the mixed $^{12}C^{16}O_2$ + $^{12}C^{18}O_2$ spectra confirms that only one O atom is involved. Hence, this species also has the VCO_2 stoichiometry. Note that both the C−O and V−O stretching frequencies of this species are higher than corresponding diatomic CO and VO frequencies, so the $OVCO^+$ cation should be considered.

Previous DFT/B3LYP calculations on the interaction of V^+ with CO_2 find that the $OVCO^+$ structure is more stable than the electrostatic (V^+)(OCO) isomer because of the very strong terminal VO^+ bond formed.[14] Our DFT calculations obtained a very similar optimized $OVCO^+$ geometry, and the C−O and V−O stretching frequencies were calculated at 2160.2 and 1095.4 cm^{-1}. The calculated isotopic ratios (C−O, 12/13, 1.02316, 16/18, 1.02423; V−O, 16/18, 1.04533) are in excellent agreement with the observed values (Table 8).

TABLE 2: Infrared Absorptions (cm^{-1}) from Co-Deposition of Laser-Ablated Ti Atoms with CO_2 in Excess Argon at 10 K

$^{12}C^{16}O_2$	$^{13}C^{16}O_2$	$^{12}C^{18}O_2$	$^{12}C^{16}O_2 + {}^{13}C^{16}O_2$	$^{12}C^{16}O_2 + {}^{12}C^{16}O/{}^{18}O + {}^{12}C^{18}O_2$	*R*(12/13)	*R*(16/18)	assignment
2344.8	2279.2	2309.7	2344.8, 2279.2	2344.8, 2327.8, 2309.7	1.02878	1.01520	CO_2
2339.0	2273.6	2304.1	2239.0, 2273.6	2239.0, 2322.0, 2304.1	1.02876	1.01515	CO_2
2193.4	2144.4	2142.5			1.02285	1.02376	$O_2Ti(CO)_2$, $\nu_{antisym}$
2190.4	2141.7	2138.3			1.02274	1.02437	O_2TiCO ?
2188.0	2138.0	2137.0			1.02339	1.02387	$OTiCO^+$
2185.5	2136.7	2134.8			1.02285	1.02381	$OTiCO^+$ site
2143.0	2095.8	2092.0	2143.0, 2095.8	2143.0, 2092.0	1.02252	1.02438	$(CO)_x$
2138.3	2091.1	2087.2	2138.3, 2091.1	2138.2, 2087.3	1.02257	1.02448	CO
2100.9	2054.7	2051.4	2101.7, 2055.6	2100.9, 2051.4	1.02249	1.02413	$TiOCO^+$?
2065.2	2019.9	2015.8	2065.2, 2019.9	2065.2, 2015.8	1.02243	1.02451	$OTiOC^+$
2037.1	1983.3				1.02713		CO_3
2027.3	1981.3	1981.2	2027.3, 2006.3, 1981.3		1.02322	1.02327	$OTi(CO)_2$, ν_{sym}
1866.8	1823.8	1825.9	1866.7, 1823.8	1866.8, 1825.8	1.02358	1.02240	OTiCO
1864.4	1821.5	1823.9	1864.4, 1821.5	1864.4, 1823.9	1.02355	1.02221	OTiCO site
1856.7	1806.4	1826.8	1856.9, 1806.7		1.02784	1.01659	$C_2O_4^-$
1833.2	1793.3	1789.3	1833.2, 1810.7, 1793.4	1833.2, 1808.6, 1789.3	1.02225	1.02453	$OTi(CO)_2$, $\nu_{antisym}$
1657.0	1612.9	1629.3	1656.9, 1612.9	1657.0, 1643.9, 1629.3	1.02734	1.01700	CO_2^-
1652.7	1608.8	1625.0	1652.8, 1608.8	1652.7, 1639.8, 1625.0	1.02728	1.01705	$(CO_2^-)(CO_2)_x$
1532.3	1496.8	1496.1	1532.4, 1496.7	1532.3, 1496.1	1.02372	1.02420	OTi[CO]
1383.9	1368.9	1339.2			1.01096	1.03338	$(CO_2)_x$
1278.4	1255.8	1227.7			1.01800	1.04130	$(CO_2)_x$
1274.0	1264.8	1221.7			1.00727	1.04281	$C_2O_4^+$
1257.0	1248.2	1200.2			1.00705	1.04733	CO_4^-
1184.7	1177.3	1130.5			1.00629	1.04794	$C_2O_4^-$
1012.9	1012.9	970.0		1012.9, 970.0		1.04423	$OTiOC^+$, TiO^+
1011.7	1011.6	968.7		1011.6, 968.8		1.04439	$TiOCO^+$
1004.3	1004.3	961.6		1004.3, 961.6		1.04441	$OTiCO^+$ site
1003.0	1003.0	960.3		1003.0, 960.3		1.04447	$OTiCO^+$
990.2	990.2						TiO site ?
987.9	987.9	946.1				1.04418	TiO
985.6	985.6	944.0				1.04407	TiO site
965.0	965.0	924.5		965.0, 924.6		1.04381	OTi[CO]
954.7	954.7	913.9		954.7, 913.9		1.04464	OTiCO site
952.8	952.8	911.3		952.6, 911.8		1.04554	OTiCO
923.1	923.1						$^{46}TiO_2$
919.9	919.9						$^{47}TiO_2$
917.0	917.0	881.6		917.0, 887.1, 881.6		1.04015	$^{48}TiO_2$
914.1	914.1						$^{49}TiO_2$
911.3	911.2						$^{50}TiO_2$
895.2	895.2	860.2		895.1, 869.6, 860.7		1.04069	O_2TiCO
888.3	888.3	854.3				1.03980	$O_2{}^{46}Ti(CO)_2$
885.4	885.4	851.2				1.04018	$O_2{}^{47}Ti(CO)_2$
882.6	882.6	848.2		882.5, 857.9, 848.2		1.04056	$O_2{}^{48}Ti(CO)_2$
879.9	879.9	845.2				1.04106	$O_2{}^{49}Ti(CO)_2$
877.3	877.3	842.9				1.04081	$O_2{}^{50}Ti(CO)_2$

$OTiCO^+$. Similar bands at 2190.4, 2185.5 and 1004.3, 1003.0 cm^{-1} in the Ti + CO_2 system exhibit analogous behavior as the $OVCO^+$ cation absorptions and are assigned to the $OTiCO^+$ cations at different sites. Agreement between the calculated and observed isotopic frequency ratios is shown in Table 8. This follows the analogous $OScCO^+$ species (Table 9) as having the highest carbonyl stretching frequency observed in each metal system.

$OVOC^+$. The 2059.3 and 1029.6 cm^{-1} bands were also produced on full arc photolysis and decreased on 30 and 35 K annealing. The upper band shifted to 2013.9 and 2010.1 cm^{-1} in $^{13}C^{16}O_2$ and $^{12}C^{18}O_2$ spectra; the 12/13 ratio, 1.02254, and 16/18 ratio, 1.02448, are extremely close to the diatomic CO ratios, and the frequency is just 21 cm^{-1} lower than the CO diatomic. In both mixed experiments, only pure isotopic counterparts were observed, indicating that this absorption is due to a weakly pertubed CO molecule. The associated 1029.6 cm^{-1} band showed no carbon-13 shift, and the 16/18 ratio 1.04507 also characterized a terminal V−O stretching vibration. These two bands are suitable for assignment to the C−O and V−O stretching vibrations of the $OVOC^+$ cation isomer analogous to the $OScOC^+$ cation.[5]

Our DFT calculations predict the $OVOC^+$ cation is only 15.6 kcal/mol higher in energy than the $OVCO^+$ cation. The V−O stretching frequency is calculated at 1102.7 cm^{-1}, 7.3 cm^{-1} higher than the $OVCO^+$ cation, while the calculated C−O stretching frequency is 1959.8 cm^{-1}, lower than the $OVCO^+$ cation, in accord with the experimental observations.

$OTiOC^+$. The bands at 1012.9 and 2065.2 cm^{-1} in the Ti + CO_2 system are assigned to the $OTiOC^+$ cation. The lower band essentially has the same frequency with the TiO^+ cation observed in an argon matrix at 1012.9 cm^{-1}. Again, Table 9 shows the relationship among the Sc, Ti, and V species.

$MOCO^+$. The 2100.9 and 2076.9 cm^{-1} bands for Ti and V follow the analogous 2105.7 cm^{-1} band for Sc; these bands all increase on full arc photolysis. The most probable assignment for these bands is to $MOCO^+$, which is essentially the $MO^+\cdots CO$ complex. This is a higher energy species than $OMCO^+$, and it may arise from rearrangement on photolysis.

The neon matrix band at 2102.7 cm^{-1} for $TiO^+\cdots CO$ shows a very small matrix difference for a cation species; however, this band is due to the vibration of the neutral CO submolecule part of the $TiO^+\cdots CO$ complex.

$O_2V(CO)_2$. Four bands at 2150.6, 2115.4, 951.3, and 942.8 cm^{-1} increased together on annealing and photolysis. The two upper bands showed C−O stretching isotopic ratios. Both mixed $^{12}C^{16}O_2 + {}^{13}C^{16}O_2$ and $^{12}C^{16}O_2 + {}^{12}C^{18}O_2$ experiments gave 1/2/1 triplets for both bands. This is indicative of the presence

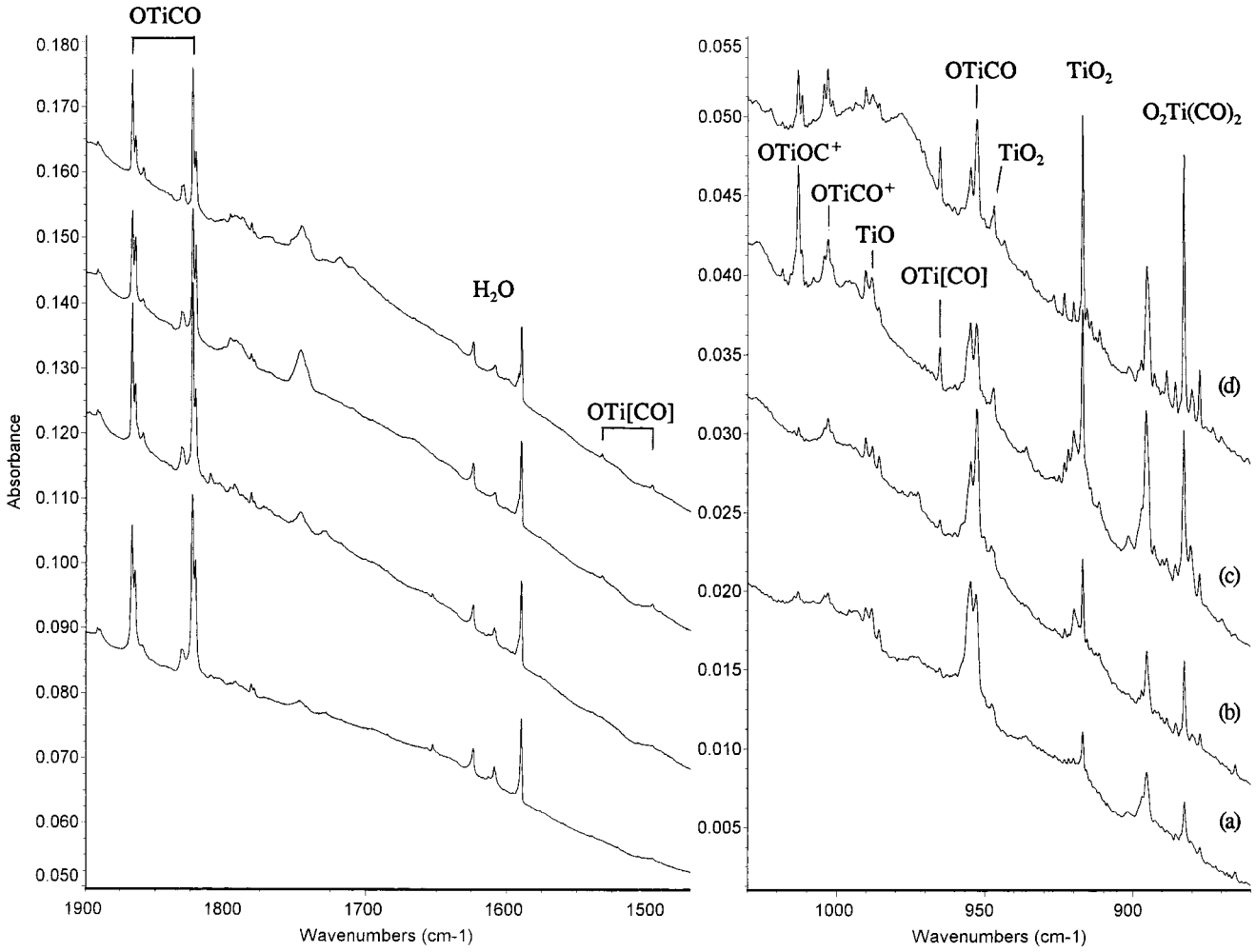

Figure 4. Infrared spectra in selected regions for reaction of laser-ablated Ti atoms with 0.25% $^{12}CO_2$ + 0.25% $^{13}CO_2$ in argon during condensation at 12 K: (a) sample co-deposition for 1 h, (b) after annealing to 25 K, (c) after 15 min broad-band photolysis, and (d) after annealing to 30 K.

of two equivalent CO groups that come from two different CO_2 molecules. While the two lower bands showed no carbon-13 shift, the isotopic 16/18 ratios of the 942.8 cm^{-1} (1.03936) and 949.8 cm^{-1} (1.0495) absorptions indicate these two bands are due to antisymmetric and symmetric OVO stretching vibrations. These four bands are assigned to the $O_2V(CO)_2$ molecule. This assignment is confirmed by DFT calculations, which predicted that $O_2V(CO)_2$ has C_{2v} symmtery with antisymmetric and symmetric C−O vibrations at 2040.8 and 2098.7 cm^{-1} and antisymmetric and symmetric VO_2 vibrations at 970.9 and 984.0 cm^{-1}, in excellent agreement with observed values.

$OV(CO)_2$. Weak bands at 1851.7 and 1984.5 cm^{-1} observed on deposition increased together on 25 K annealing. The 1851.6 cm^{-1} band shifts to 1810.1 and 1808.8 cm^{-1} in $^{13}C^{16}O_2$ and $^{12}C^{18}O_2$ spectra and gives C−O stretching isotopic ratios (12/13, 1.02293, and 16/18, 1.02361). The 1984.5 cm^{-1} band showed a slightly higher 12/13 ratio (1.02336) and lower 16/18 ratio (1.02304) than the 1851.6 cm^{-1} band, indicating more C and less O anticipation. In both mixed $^{12}C^{16}O_2$ + $^{13}C^{16}O_2$ and $^{12}C^{16}O_2$ + $^{12}C^{18}O_2$ experiments, triplets with 1/2/1 intensity distribution were produced, so two equivelant CO subunits are involved in this molecule. These two bands are not due to $V(CO)_2$ complexes.[31] The lower band is below while the upper band is above ν(CO) for the OVCO molecule, so the $OV(CO)_2$ molecule is suggested. DFT calculation of $OV(CO)_2$ gave strong antisymmetric and symmetric C−O vibrations at 1941.3 and 1990.7 cm^{-1}, in excellent agreement with observed values. This calculation predicted the V−O stretching vibration at 972.1 cm^{-1} with about 10% intensity of antisymmetric C−O vibration, and this weaker mode is not observed here.

$O_2Ti(CO)$, $O_2Ti(CO)_2$. In the Ti + CO_2 reaction, two bands at 882.6 and 895.2 cm^{-1} increased on annealing and photolysis; both bands show no carbon-13 shifts and antisymmetric OTiO stretching ratios. The Ti isotopic splitting of the lower band is clear, for only one Ti atom involvment. Two bands at 2193.4, 2188.0 cm^{-1} track with these two absorptions. These bands are probably due to the $O_2Ti(CO)$ and $O_2Ti(CO)_2$ molecules. According to the DFT calculations listed in Table 6, the 882.6 and 2193.4 cm^{-1} bands are due to the $O_2Ti(CO)_2$ molecule, while the 895.2 and 2188.0 cm^{-1} bands are due to the $O_2Ti(CO)$ molecule.

$OTi(CO)_2$. Weak bands at 1833.2 and 2027.3 cm^{-1} increased on annealing. Both bands exhibit C−O stretching vibrational ratios; in the mixed experiments, 1/2/1 triplets were observed, so two equivalent CO subunits were involved. These two bands are assigned to the $OTi(CO)_2$ molecule. Again, the Ti−O vibration was too weak to be observed as our DFT calculation predicted.

Counterions. In addition to the $OMCO^+$, $OMOC^+$, and $MOCO^+$ cations identified here, counteranions must be present to maintain the overall charge neutrality of the matrix sample. There is no evidence for metal-containing anions in the Sc, Ti, and V experiments; however, the $OMCO^-$ anions have been observed in laser-ablation experiments with later transition metal atoms.[30] All samples contain CO_2^- at 1657.0 cm^{-1}, which on annealing converts to $C_2O_4^-$ absorbing at 1857.1 and 1184.7

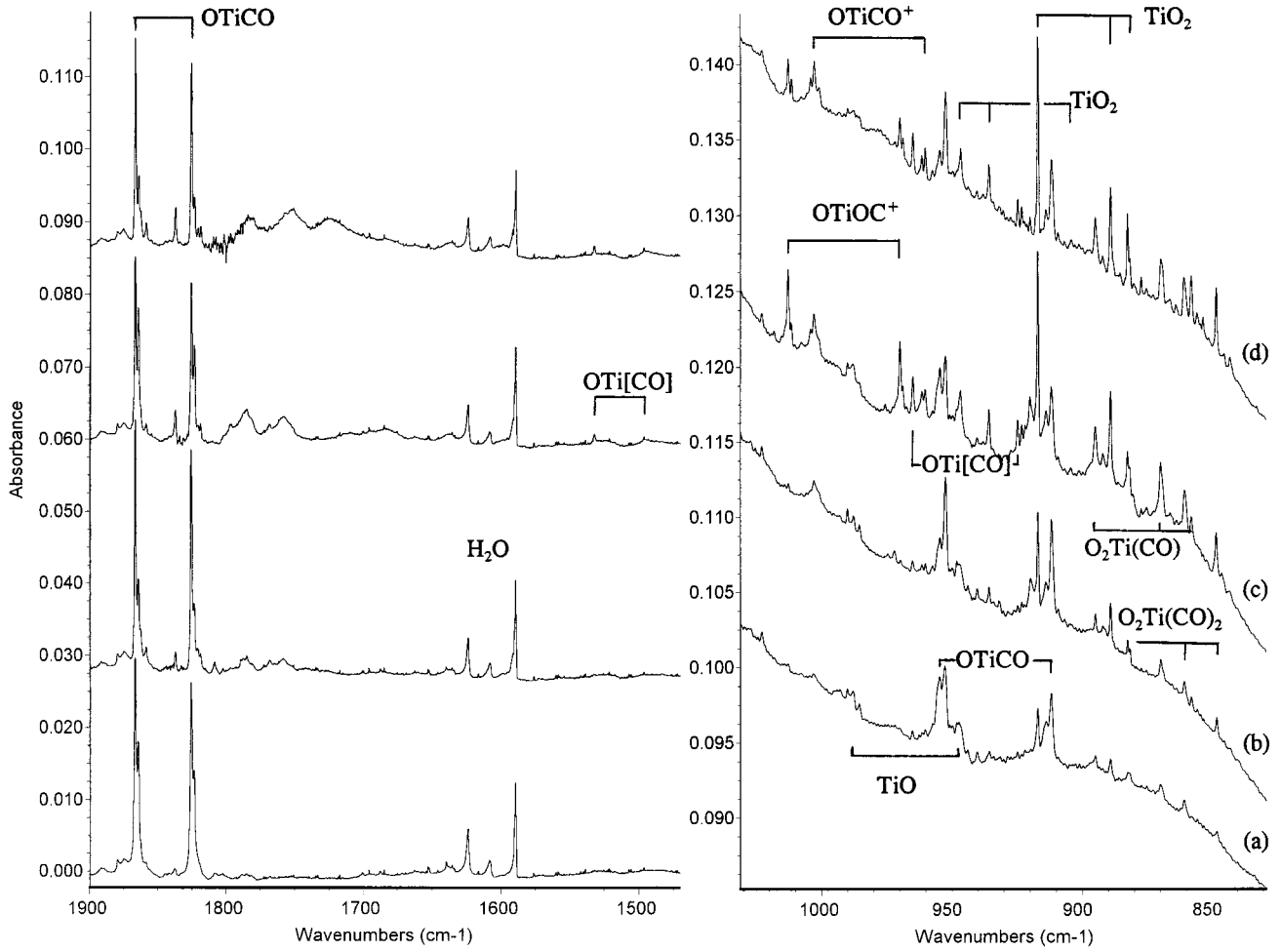

Figure 5. Infrared spectra in selected regions for reaction of laser-ablated Ti atoms with 0.6% statistical $C^{16}O_2 + C^{16}O^{18}O + C^{18}O_2$ in argon during condensation at 12 K. (a) sample co-deposition for 1 h; (b) after annealing to 25 K, (c) after 15 min broad-band photolysis; (d) after annealing to 30 K.

TABLE 3: Infrared Absorptions (cm^{-1}) from Co-Deposition of Laser-Ablated Ti Atoms with CO_2 in Excess Neon at 4 K

$^{12}C^{16}O_2$	$^{13}C^{16}O_2$	$^{12}C^{18}O_2$	*R*(12/13)	*R*(16/18)	assignment	$^{12}C^{16}O_2$	$^{13}C^{16}O_2$	$^{12}C^{18}O_2$	*R*(12/13)	*R*(16/18)	assignment
2347.3	2291.9	2312.4	1.02866	1.01509	CO_2	1654.6	1610.6	1626.9	1.02732	1.01703	$(CO_2^-)(CO_2)_2$
2216.8	2167.2	2165.2	1.02289	1.02383	?	1650.5	1606.9	1623.0	1.02713	1.01694	$(CO_2^-)(CO_2)$
2196.3	2147.3	2145.3	1.02282	1.02377	$O_2Ti(CO)_2$	1539.0					OTi[CO]
2193.4	2144.5	2142.3	1.02280	1.02385	$O_2Ti(CO)_2$ site	1421.6	1380.3	1399.6	1.02992	1.01572	CO_2^+
2146.1	2098.5	2095.1	1.02268	1.02434	$(CO)_x$	1274.4	1262.9	1227.4	1.00911	1.03829	$C_2O_4^+$
2140.8	2093.7	2098.7	1.02250	1.02445	CO	1189.2	1181.4	1135.4	1.00660	1.04738	$C_2O_4^-$
2130.8	2074.5		1.02714		$(C_2O_4^+)$	1185.9	1178.5	1133.0	1.00628	1.04669	$C_2O_4^-$ site
2102.7	2056.3	2052.3	1.02256	1.02456	$TiOCO^+$?	1183.7	1176.4	1129.7	1.00621	1.04780	$C_2O_4^-$ site
1884.0	1841.0	1842.1	1.02336	1.02275	OTiCO	1041.5	1018.9	1024.8	1.02218	1.01630	Ti[OO]CO
1862.1	1812.0	1830.3	1.02765	1.01737	$C_2O_4^-$ site	997.6	997.6	955.3		1.04428	TiO
1854.8		1823.1		1.01739	$C_2O_4^-$ site	990.6	990.6	949.7		1.04307	OTi[CO]
1852.3	1802.9	1820.8	1.02740	1.01730	$C_2O_4^-$	973.1	973.1	931.5	1.00031	1.04466	OTiCO
1829.5	1789.2	1785.4	1.02252	1.02470	$OTi(CO)_2$	936.4	936.4	900.3		1.04010	TiO_2
1800.9	1754.2	1765.7	1.02662	1.01994	Ti[OO]CO	906.1	906.1	870.9		1.04042	$O_2Ti(CO)$
1670.0	1625.5	1642.3	1.02738	1.01687	$(CO_2)_2(CO_2^-)$	892.9	892.9	858.1		1.04055	$O_2Ti(CO)_2$
1665.3	1621.0	1637.6	1.02733	1.01691	$(CO_2)(CO_2^-)$	891.7	891.7	856.8		1.04073	$O_2Ti(CO)_2$ site
1658.2	1614.1	1630.6	1.02732	1.01693	CO_2^-	679.2	664.8		1.02166		$C_2O_4^-$

cm^{-1}.[18,19] In addition, CO_4^- is observed at 1257.0 and 691.3 cm^{-1},[19,32] and a weak metal-independent CO_3 band at 2037.1 cm^{-1} increased on full arc photolysis.[32] Finally, the metal-independent band at 1274.0 cm^{-1} will be identified as $C_2O_4^+$ in a future report.[33]

Reaction Mechanisms. Laser-ablated V and Ti atoms insert into CO_2 to form the OMCO molecules, reaction 1, which is the dominant process. This is also the case for Cr, Mn, Fe, Co and Ni atoms.[30] Recent calculations show that there is no energy barrier for ground-state Ti atom insertion into CO_2 to form the OTiCO molecule.[16] The OMCO molecule can further react with another CO_2 molecule to form the stable dioxide complex $O_2M(CO)_2$, reaction 2.

$$V + CO_2 \rightarrow OVCO \quad (1a)$$

$$Ti + CO_2 \rightarrow OTiCO \quad (1b)$$

$$OVCO + CO_2 \rightarrow O_2V(CO)_2 \quad (2a)$$

$$OTiCO + CO_2 \rightarrow O_2Ti(CO)_2 \quad (2b)$$

TABLE 4: Calculated (BP86/6-311+G*) Geometry, Relative Energies (kcal/mol), Vibrational Frequencies (cm^{-1}), and Intensities (km/mol) for VCO_2 and VCO_2^+ Isomers

molecule	relative energy	geometry	frequency (intensity)
OVCO ($^4A''$)	0	V−O, 1.605 Å; V−C, 2.007 Å; C−O, 1.161 Å; ∠OVC, 108.8°; ∠VCO, 164.7°	1959.8 (1173), 981.1 (197), 415.4 (7), 338.5 (2), 292.6 (0), 130.6 (10)
OVCO ($^2A''$)	+8.7	V−O, 1.580 Å; V−C, 1.916 Å; C−O, 1.171 Å; ∠OVC, 98.4°, ∠VCO, 176.6°	1893.9 (2050), 1046.9 (174), 457.4 (76), 336.7 (94), 331.3 (14), 153.0 (4)
OV[CO′] ($^2A''$)	+21.8	V−O:1.592 Å; V−C:2.030 Å; V−O′:2.007 Å; C−O′:1.239 Å; ∠OVC, 114.1°, ∠OVO′:121.6°, ∠CVO′:35.7°	1489.6 (561), 1023.6 (167), 476.3 (25), 366.7 (24), 194.3 (24), 144.1 (48)
V[OC]O′ ($^4A'$)	+27.2	V−O:1.819 Å; V−C:1.976 Å; C−O:1.402 Å; C−O′:1.200 Å; ∠OVC, 43.1°, ∠OCO′:129.4°	1769.2 (585), 849.0 (137), 655.6 (26), 423.7 (9), 362.8 (0.6), 320.9 (10)
V[OC]O′ ($^6A'$)	+38.7	V−O:2.088 Å; V−C:2.210 Å; C−O:1.247 Å; C−O′:1.195 Å; ∠OVC, 33.6°, ∠OCO′:150.1°	1960.7 (384), 1139.7 (173), 622.9 (240), 432.0 (0.5), 348.1 (4), 194.5 (3)
V[OO]C ($^4B_1$)	+42.4	V−O:1.897 Å; C−O:1.338 Å; ∠OVO:71.7°, ∠OCO:112.3°	1014.8 (101), 978.5 (330), 453.0 (131), 404.5 (32), 370.0 (7), 75.2 (31)
VOCO′ ($^6A'$)	+44.8	V−O:2.097 Å; O−C:1.185 Å; C−O′:1.175 Å; ∠VOC:174.5°, ∠OCO′:179.8°	2334.3 (787), 1229.6 (289), 367.8 (14), 365.5 (14), 211.3 (12), 54.9 (1)
VCO_2 ($^6A_2$)	+48.5	V−C:2.302 Å; C−O:1.209 Å; ∠OCO:154.4°	2003.8 (244), 1186.2 (230), 568.6 (440), 448.4 (1), 84.9 (0.4), 36.5i (7)
$OVCO^+$ ($^3A'$)	+169.2	V−O:1.553 Å; V−C:2.125 Å; C−O:1.133 Å; ∠OVC, 101.7°, ∠VCO, 172.4°	2160.2 (250), 1095.4 (92), 332.4 (1), 282.1 (0.1), 269.2 (1), 114.0 (16)
$OVO'C^+$ ($^3A'$)	+184.8	V−O:1.552 Å; V−O′:2.150 Å; C−O′:1.159 Å; ∠OVO′:114.2°, ∠VO′C:171.1°	1959.8 (119), 1102.7 (96), 266.1 (13), 175.7 (5), 165.8 (6), 85.1 (18)
$VOCO^+$ ($^3\Sigma^-$)	+187.2	V−O:1.547 Å; O−C:3.781 Å; C−O:1.143 Å; ∠VOC:180°, ∠OCO:180°	2137.1 (73), 1110.4 (65), 44.0 (7), 13.3 (6), 18.5i (23)

TABLE 5: Calculated (BP86/6-311+G*) Geometry, Relative Energies (kcal/mol), Vibrational Frequencies (cm^{-1}), and Intensities (km/mol) for $TiCO_2$ and $TiCO_2^+$ Isomers

molecule	relative energy	geometry	frequency (intensity)
OTiCO ($^3A'$)	0	Ti−O, 1.625 Å; Ti−C, 2.094 Å; C−O, 1.158 Å; ∠OTiC, 98.1°, ∠TiCO, 176.4°	1965.1(1696), 989.3 (189), 380.5 (24), 321.4 (32), 260.5 (1), 106.7 (2)
OTiCO ($^1A'$)	+6.5	Ti−O, 1.629 Å; Ti−C, 1.989 Å; C−O, 1.179 Å; ∠OTiC, 101.2°, ∠TiCO, 178.6°	1882.1 (616), 987.7 (190), 478.3 (2), 347.3 (0.3), 292.4 (48), 134.3 (15)
OTi[CO′] ($^1A'$)	+11.2	Ti−O, 1.626 Å; Ti−C, 2.085 Å; Ti−O′, 2.004 Å; C−O′, 1.246 Å; ∠OTiC, 107.0°, ∠OTiO′, 108.8°, ∠CTiO′, 35.4°	1483.4 (189), 1000.5 (190), 459.3 (2), 451.9 (7), 254.5 (7), 209.5 (15)
OTi[CO′] ($^3A'$)	+14.8	Ti−O, 1.622 Å; Ti−C, 2.255 Å; Ti−O′, 2.198 Å; C−O′, 1.197 Å; ∠OTiC, 103.4°, ∠OTiO′, 112.8°, ∠CTiO′, 31.1°	1681.4 (761), 998.0 (232), 354.2 (19), 290.4 (20), 177.3 (7), 126.1 (12)
Ti[OO]C ($^3B_1$)	+35.8	Ti−O, 1.885 Å; O−C, 1.358 Å; ∠OTiO, 73.6°, ∠OCO, 112.5°	994.2 (31), 952.6 (310), 696.8 (4), 473.4 (30), 341.1 (3), 293.2 (38)
Ti[OC]O′ ($^5A'$)	+50.8	Ti−O, 2.154 Å; Ti−C, 2.250 Å; C−O, 1.249 Å; C−O′, 1.199 Å; ∠OTiC, 32.9°, ∠OCO′, 148.8°	1932.7 (339), 1145.1 (190), 636.3 (239), 481.2 (1), 326.7 (1), 187.8 (2)
$OTiCO^+$ ($^2A'$)	+156.7	Ti−O, 1.588 Å; Ti−C, 2.168 Å; C−O, 1.136 Å; ∠OTiC, 94.5°, ∠TiCO, 174.9°	2139.5 (301), 1070.8 (112), 356.2 (4), 315.1 (1), 268.0 (3), 125.9 (21)
$OTiO'C^+$ ($^2A'$)	+172.0	Ti−O, 1.586 Å; Ti−O′, 2.192 Å; C−O′, 1.159 Å; ∠OTiO′, 105.9°, ∠TiO′C, 174.1°	1950.1 (55), 1077.1 (124), 263.1 (15), 187.4 (7), 182.7 (6), 95.9 (21)
$TiOCO^+$ ($^2\Delta$)	+187.2	Ti−O, 1.580 Å; O−C, 4.643 Å; C−O, 1.159 Å; ∠TiOC, 180°, ∠OCO, 180°	2132.6 (71), 1089.1 (105), 35.5 (7), 13.3 (5), 19.3i (33)

TABLE 6: Calculated Geometries, C−O and V−O Vibrational Frequencies (cm^{-1}), and Intensities (km/mol) for $OV(CO)_2$, $O_2V(CO)$, and $O_2V(CO)_2$ Molecules

molecule	geometry	sym C−O	antisym C−O	sym V−O	antisym V−O
$OV(CO)_2$ ($^4A''$)	V−O, 1.616 Å; V−C, 2.03 Å; C−O, 1.158 Å; ∠OVC, 114.3°, ∠CVC, 97.7°, ∠VCO, 164.1°	1990.7 (753)	1941.3 (1578)	972.1 (163)	
O_2VCO ($^2B_1$)	V−O, 1.622 Å; V−C, 2.037 Å; C−O, 1.149 Å; ∠OVC, 103.0°, ∠OVO, 115.6°, ∠VCO, 170.4°	2045.8 (769)		983.2 (56)	968.4 (262)
$O_2V(CO)_2$ ($^2A_1$)	V−O, 1.623 Å; V−C, 2.082 Å; C−O, 1.145 Å; ∠OVC, 108.7°, ∠CVC, 104.7°, ∠VCO, 175.8°, ∠OVO, 116.8°	2098.7 (267)	2040.8 (1205)	984.0 (42)	970.9 (215)

The OM−(η^2-CO) molecules were produced on full arc photolysis, which suggests photoisomerization reaction 3, which was calculated to be slightly endothermic (M = Ti, V).

$$\mathrm{OMCO} + h\nu \rightarrow \mathrm{OM}-(\eta^2\text{-CO}) \qquad (3)$$

The $OMCO^+$ and $OMOC^+$ cations were also produced on full arc photolysis. As has been discussed,[5] these cations are probably formed by photoexcitation and photoionization of OM−(η^2-CO) molecules via a long-lived OM−(η^2-CO)* excited state, reaction 4,

$$\mathrm{OM}-(\eta^2\text{-CO}) + h\nu \rightarrow \mathrm{OM}-(\eta^2\text{-CO})^* + h\nu \rightarrow \mathrm{OMCO}^+ \text{ or } \mathrm{OMOC}^+ + \mathrm{e}^- \qquad (4)$$

The role of CCl_4 dopant in these experiments is to capture electrons produced in the ablation process and in reaction 4, which facilitates the survival of cations, such as the products of reaction 4, as described previously.[34]

TABLE 7: Calculated Geometries, C−O and Ti−O Vibrational Frequencies(cm^{-1}), and Intensities (km/mol) for $OTi(CO)_2$, $O_2Ti(CO)$ and $O_2Ti(CO)_2$ Molecules

molecule	geometry	sym C−O	antisym C−O	sym Ti−O	antisym Ti−O
$OTi(CO)_2$ ($^3A''$)	Ti−O, 1.631 Å; Ti−C, 2.122 Å; C−O, 1.159 Å; ∠OTiC, 108.1°, ∠CTiC, 119.2°, ∠TiCO, 174.5°	2000.5 (217)	1929.6 (2113)	984.6 (185)	
O_2TiCO ($^1A'$)	Ti−O, 1.667 Å; V−C, 2.200 Å; C−O, 1.139 Å; ∠OTiC, 89.8°, ∠OTiO, 109.2°, ∠TiCO, 168.5°	2127.7 (346)		957.5 (29)	892.3 (268)
$O_2Ti(CO)_2$ ($^1A_1$)	V−O, 1.623 Å; V−C, 2.082 Å; C−O, 1.145 Å; ∠OVC, 108.7°, ∠CVC, 104.7°, ∠VCO, 175.8°, ∠OVO, 116.8°	2142.3 (25)	2127.4 (787)	940.8 (24)	864.9 (214)

TABLE 8: Comparison of Observed and Calculated Vibrational Frequencies and Isotopic Frequency Ratios for OMCO, OM−(η^2-CO), $OMCO^+$, and $OMOC^+$ Species (M = V,Ti)

molecule	obsd	calcd	12/13 obsd	12/13 calcd	16/18 obsd	16/18 calcd
OVCO ($^4A''$)	1881.1	1959.8	1.02356	1.02334	1.02261	1.02393
	974.8	981.1	1.00000	1.00000	1.04592	1.04539
OVCO ($^2A'$)		1893.9		1.02345		1.02373
		1046.9		1.00000		1.04523
OV−(η^2-CO)	1516.1	1489.6	1.02227	1.02195	1.02431	1.02561
	990.0	1023.6	1.00000	1.00000	1.04485	1.04502
$OVCO^+$	2205.4	2160.2	1.02282	1.02316	1.02391	1.02423
	1020.0	1095.4	1.00000	1.00000	1.04508	1.04533
$OVOC^+$	2059.3	1959.8	1.02254	1.02341	1.02448	1.02382
	1029.6	1102.7	1.00000	1.00000	1.04507	1.04521
OTiCO ($^3A''$)	1866.8	1965.1	1.02358	1.02328	1.02240	1.02408
	952.8	989.3	1.00000	1.00000	1.04554	1.04467
OTiCO ($^1A'$)		1882.1		1.02383		1.02316
		987.7		1.00000		1.04452
OTi−(η^2-CO)	1532.3	1483.4	1.02372	1.02254	1.02420	1.02487
	965.0	1000.5	1.00000	1.00000	1.04381	1.04436
$OTiCO^+$	2190.4	2139.5	1.02274	1.02310	1.02437	1.02427
	1003.0	1070.8	1.00000	1.00000	1.04441	1.04468
$OTiOC^+$	2065.2	1950.1	1.02243	1.02303	1.02451	1.02437
	1012.9	1077.1	1.00000	1.00000	1.04423	1.04451

TABLE 9: Comparison of Infrared Absorptions for Reaction Products of Laser-Ablated Early Transition Metal Atoms with CO_2

product	Sc	Ti	V	Cr	Mn
$OMCO^+$	221.8	2188.0	2205.4	2175.5	2173.0
	965.5	1003.0	1020.0		851.9
$O_2M(CO)_2$			2150.6	2123.2	2126.0
		2193.4	2115.4	2059.7	2056.0
		828.6	947.8	981.4	993.8
$MOCO^+$	2105.7	2100.9	2076.9		
	976.4				
$OMOC^+$	2068.1	2065.2	2059.3		
	974.1	1012.9	1029.6		
$OM(CO)_2$		2027.3	1984.5	1923.9	1929.9
		1833.2	1851.6		
OMCO	1873.4	1866.8	1881.1	2014.4	2082.5
	894.1	952.8	974.8	866.3	869.9
OM[CO]	1613.9	1532.3	1516.1		
	906.6	965.0	988.1		
$OMCO^-$				1831.1	1810.0
				825.5	810.1

Conclusions

Laser-ablated V and Ti atoms react with CO_2 molecules to give primarily the insertion products, OMCO and $O_2M(CO)_2$, which have been isolated in a solid argon matrix. Similar neon matrix experiments with Ti and CO_2 give these products with modest matrix shifts. Photoisomerization of OMCO molecules to form the side-bonded OM−(η^2-CO) isomers and photoionization to give the $OMCO^+$ and $OMOC^+$ cations and the $MO^+\cdot\cdot\cdot$CO cation complex proceed upon mercury arc photolysis. The product absorptions were identified by isotopic substitution and density functional calculations of isotopic frequencies. In addition, the molecular anions CO_2^-, CO_4^-, and $C_2O_4^-$ were observed in these experiments. Although CO_2^- was trapped in both solid argon and neon, $C_2O_4^-$ was formed during condensation in neon but annealing was required to produce $C_2O_4^-$ in solid argon.

Acknowledgment. We gratefully acknowledge NSF support for this research under grant CHE 97-00116.

References and Notes

(1) Gibson, D. H. *Chem. Rev.* **1996**, *96*, 2063.
(2) Mascetti, J.; Tranquille, M. *J. Phys. Chem.* **1988**, *92*, 2173.
(3) Chertihin, G. V.; Andrews, L. *J. Am. Chem. Soc.* **1995**, *117*, 1595.
(4) Souter, P. S.; Andrews, L. *J. Am. Chem. Soc.* **1997**, *119*, 7350.
(5) Zhou, M. F.; Andrews, L. *J. Am. Chem. Soc.* **1998**, *120*, 13230.
(6) Lessen, D. E.; Asher, R. L.; Brucat, P. J. *J. Chem. Phys.* **1991**, *95*, 1414.
(7) Schwartz, J.; Schwartz, H. *Organometallics* **1994**, *13*, 1518.
(8) Schwartz, J.; Heinemann, C.; Schwartz, H. *J. Phys. Chem.* **1995**, *99*, 11405.
(9) Sievers, M. R.; Armentrout, P. B. *J. Chem. Phys.* **1995**, *102*, 754.
(10) Asher, R. L.; Bellert, D.; Buthelezi, T.; Brucat, P. J. *Chem. Phys. Lett.* **1994**, *227*, 623. Asher, R. L.; Bellert, D.; Buthelezi, T.; Weerasekera, G.; Brucat, P. J. *Chem. Phys. Lett.* **1994**, *228*, 390.
(11) Baranov, V.; Javahery, G.; Hopkinson, A. C.; Bohme, D. K. *J. Am. Chem. Soc.* **1995**, *117*, 12801.
(12) Sodupe, M.; Branchadell, V.; Oliva, A. *J. Phys. Chem.* **1995**, *99*, 8567.
(13) Jeung, G. H. *Chem. Phys. Lett.* **1995**, *232*, 319.
(14) Sodupe, M.; Branchadell, V.; Rosi, M.; Bauschlicher, C. W., Jr. *J. Phys. Chem. A* **1997**, *101*, 7854
(15) Galan, F.; Fouassier, M.; Tranquille, M.; Mascetti, J.; Papai, I. *J. Phys. Chem. A* **1997**, *101*, 2626.
(16) Papai, I.; Mascetti, J.; Fournier, R. *J. Phys. Chem. A* **1997**, *101*, 4465.
(17) (a) Burkholder, T. R.; Andrews, L. *J. Chem. Phys.* **1991**, *95*, 8697, (b) Hassanzadeh, P.; Andrews, L. *J. Phys. Chem.* **1992**, *96*, 9177.
(18) Jacox, M. E.; Thompson, W. E. *J. Chem. Phys.* **1989**, *91*, 1410.
(19) Zhou, M. F.; Andrews, L. *J. Chem. Phys.* **1999**, *110*, 2414.
(20) Chertihin, G. V.; Andrews, L. *J. Phys. Chem.* **1995**, *99*, 6356.
(21) Jacox, M. E.; Milligan, D. H. *J. Chem. Phys.* **1971**, *54*, 3935.
(22) Prochaska, F. T.; Andrews, L. *J. Chem. Phys.* **1977**, *67*, 1091.
(23) Menberger, L. *Ber. Bunsen-Ges. Phys. Chem.* **1982**, *86*, 252. Matejeik, S.; Kiendler, A.; Stamatovic, A.; Mark, T. D. *Int. J. Mass. Spectrom. Ion Processes* **1995**, *149/150*, 311.
(24) Frisch, M. J.; Trucks, G. W.; Schlegel, H. B.; Gill, P. M. W.; Johnson, B. G.; Robb, M. A.; Cheeseman, J. R.; Keith, T.; Petersson, G. A.; Montgomery, J. A.; Raghavachari, K.; Al-Laham, M. A.; Zakrzewski, V. G.; Ortiz, J. V.; Foresman, J. B.; Cioslowski, J.; Stefanov, B. B.; Nanayakkara, A.; Challacombe, M.; Peng, C. Y.; Ayala, P. Y.; Chen, W.; Wong, M. W.; Andres, J. L.; Replogle, E. S.; Gomperts, R.; Martin, R. L.; Fox, D. J.; Binkley, J. S.; Defrees, D. J.; Baker, J.; Stewart, J. P.; Head-Gordon, M.; Gonzalez, C.; Pople, J. A. *Gaussian 94*, Revision B.1; (Gaussian, Inc.: Pittsburgh, PA, 1995.
(25) Perdew, J. P. *Phys. Rev. B* **1986**, *33*, 8822. Becke, A. D. *J. Chem. Phys.* **1993**, *98*, 5648.
(26) McLean, A. D.; Chandler, G. S. *J. Chem. Phys.* **1980**, *72*, 5639. Krishnan, R.; Binkley, J. S.; Seeger, R.; Pople, J. A. *J. Chem. Phys.* **1980**, *72*, 650.
(27) Wachters, J. H. *J. Chem. Phys.* **1970**, *52*, 1033. Hay, P. J. *J. Chem. Phys.* **1977**, *66*, 4377.
(28) Chertihin, G. V.; Bare, W. D.; Andrews, L. *J. Phys. Chem. A* **1997**, *101*, 5090.
(29) Scott, A. P.; Radom, L. *J. Phys. Chem.* **1996**, *100*, 16502.
(30) Zhou, M. F.; Liang, B. Y.; Andrews, L. *J. Phys. Chem. A* **1999**, *103*, 2013.
(31) Hanlan, L.; Huber, H.; Ozin, G. A. *Inorg. Chem.* **1976**, *15*, 2592.
(32) Jacox, M. E.; Thompson, W. E. *J. Phys. Chem.* **1991**, *95*, 2781.
(33) Zhou, M. F.; Andrews, L. *J. Chem. Phys.*, in press. ($C_2O_4^+$ in neon).
(34) Zhou, M. F.; Chertihin, G. V.; Andrews, L. *J. Chem. Phys.* **1998**, *109*, 10893.